J Mol Model (2012) 18:2399–2408
DOI 10.1007/s00894-011-1239-5

ORIGINAL PAPER

How to simulate affinities for host–guest systems lacking binding mode information: application to the liquid chromatographic separation of hexabromocyclododecane stereoisomers

Vedat Durmaz · Marcus Weber · Roland Becker

Received: 5 July 2011 / Accepted: 7 September 2011 / Published online: 12 October 2011
© Springer-Verlag 2011

Abstract A novel approach for the simulation of host–guest systems by systematically scanning the host molecule's orientations within the guest cavity is presented along with a thermodynamic strategy for determining preferential binding modes and corresponding optimal interaction energies between host and guest molecules. By way of example, the elution order of hexabromocyclododecane stereoisomers from high performance liquid chromatography separation on a permethylated β-cyclcodextrin stationary phase has been computed using classical molecular dynamics simulations with the explicit solvents water and acetonitrile. Comparison of estimated with experimental separation data reveals remarkable squared coefficients of correlation with R^2=0.87 and a very high correlation $R_{\mathrm{LOO}^2} = 0.72$ using the leave-one-out cross-validation method and water as solvent. In particular, the approach presented shapes up as very robust in terms of the evaluated time range under consideration, reflecting well thermodynamic equilibria. These and further observations correlating with experimental results suggest the suitability of the underlying force fields and our multi-mode approach for the estimation of relative binding affinities for host–guest systems with unknown binding modes.

Keywords Molecular simulation · Molecular dynamics · Binding affinity · Elution order · β-Cyclcodextrin

V. Durmaz (✉) · M. Weber
ZIB Zuse-Institut Berlin,
Takustraße 7,
14195 Berlin, Germany
e-mail: durmaz@zib.de

R. Becker
BAM Bundesanstalt für Materialforschung und -prüfung,
Richard-Willstätter-Straße 11,
12489 Berlin, Germany

Introduction

High performance liquid chromatography (HPLC) is a well-established method in analytical chemistry used for the decomposition of chemical mixtures. Basically, the chromatographic elution order of analytes depends only on their binding affinities to the stationary phase. From a thermodynamic point of view, the binding affinity is considered as the ratio of the concentrations of two states of a host–guest system at chemical equilibrium: the bound and the unbound state. The affinity can in turn be derived from the free energy difference of both states incorporating the system's inner energy difference as well as its entropic difference, which can both be computed by molecular dynamics (MD) simulations. In recent years, a number of different methods to estimate binding free energies or elution orders have been presented. A mathematical model for estimating enantiomeric resolutions from molecular mechanics simulations of chiral separations was developed by Zhang et al. [1]. Issaraseriruk et al. [2] derived binding free energies for enantiomeric separation with a combination of molecular docking using AutoDock [3] and semi-empirical Parametric Model 3 (PM3) [4] calculations. The latter method had substantially more discriminating power than AutoDock energies [2]. Pérez-Garrido et al. achieved excellent correlations and cross-validation values with a quantitative structure-activity relationship (QSAR) model used to predict complexation of a series of organic molecules with β-cyclodextrin (β-CD) [5]. Of course, MD simulations have been employed in order to describe guest–host interactions and separation phenomena as well [6]. All the above mentioned models for the simulation of elution orders concentrate on modelling the interaction between the compound and the stationary phase of the system, but do not include the mobile phase explicitly. This also holds for

MD investigations of chromatographic separation systems either modelled in gas phase only [7] or incorporating solvents only implicitly as published recently [6]. However, to date, many solvents still cannot be modelled implicitly. This article discusses different aspects of explicit solvent simulations of the interaction between the compounds and the stationary phase of HPLC.

On the one hand, the suitability of the underlying force field and two solvent models will be evaluated. If they are applicable, the simulated data is assumed to comprise all necessary information describing the host–guest interaction. To that effect, only physically meaningful force field terms will be extracted from the data in accordance with thermodynamic principles. In the course of comparing three algorithms for the description of the retention behavior, we will in particular check energies averaged over MD time ranges against single-step energies as known from ordinary molecular docking. Besides, and in contrast to the mainstream trend, a high value is set on consistency in the observations. Appropriate correlations of simulated with experimental results are thought to be robust regarding the time range under consideration, especially since we are simulating molecular systems at chemical equilibrium. In order to illustrate our procedure, we use by way of example the separation of hexabromocyclododecane (HBCD) stereoisomers on a permethylated β-CD stationary phase (β-pmCD).

The compound 1,2,5,6,9,10-hexabromocyclododecane (HBCD) is used widely as a brominated flame retardant (BFR) additive in upholstery textiles and polystyrene foams (EPS, XPS) in building insulation, varying in percentage between 0.8 and 4 [8–10]. In the face of a world market demand of about 22,000 metric tons [10], HBCD is one of the most high volume BFRs. It is regarded as a persistent organic pollutant (POP) and has been detected increasingly in environmental niches [11, 12] and biota including humans [13]. Recent literature on HBCD contamination in marine fish and in birds' eggs is comprehensively cited in [14] and [15], respectively. Furthermore, HBCD and its metabolites are suspected to cause endocrine disruption due to competition with thyroxine for binding to the human transthyretin receptor [16–18]. Technical HBCD consists mainly of three diastereomeric pairs of enantiomers (±)-α-, (±)-β-, (±)-γ-HBCD with the γ-diastereomer being the main component [19]. In contrast, the HBCD patterns in biota display predominantly the α-diastereomer [11–15, 20–22]. As the trace levels of HBCD in biota display a chiral signature [14, 15, 20–22], the quantification of enantiomers is of specific interest.

The separation of the six major HBCD stereoisomers (Fig. 1) by HPLC using a chiral β-pmCD phase and a water/acetonitrile (ACN) gradient was accomplished from the technical mixture [20, 23, 24] and various biota [20–22]. The analytical challenge was described conclusively with the assignment of the absolute configurations of the enantiomers by Köppen et al. [23]. In short, an analytical column with permethylated β-pmCD (NUCLEODEX β-PM) as the stationary phase (see Fig. 3) was used with a water/ACN gradient. The separation of enatiomeric pairs on this phase is possible due to the chiral nature of β-pmCD. Because of the hydrophobic character of HBCD, its interaction with β-pmCD increases in contact with water. In contrast to water, the less polar co-eluent ACN reduces guest–host interactions and thus enhances HBCD elution. The associated chromatogram from [23] is depicted in Fig. 2. HBCD was taken as example for the novel approach outlined in the following because it displays a complex cohort of diastereomers and enantiomers and is therefore regarded as ideal starting point in terms of computational challenge and practical significance.

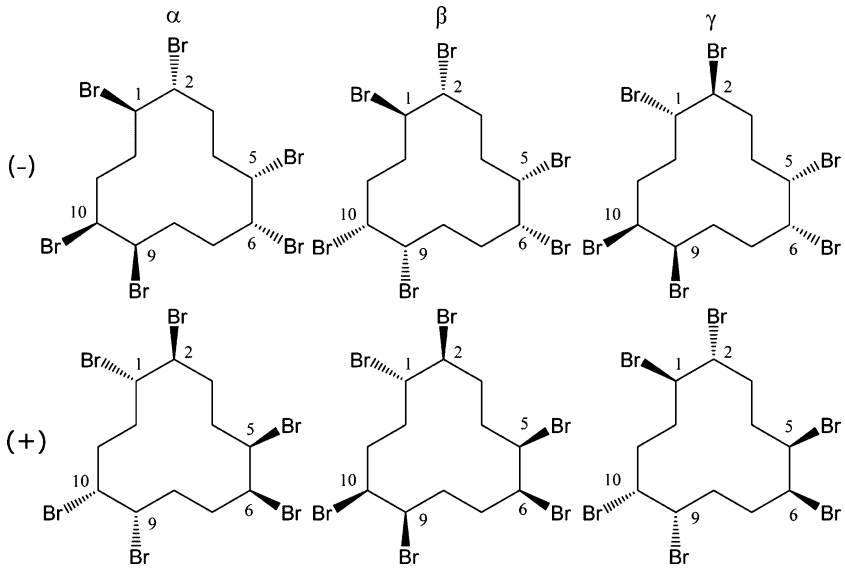

Fig. 1 The six major 1,2,5,6,9,10-hexabromocyclododecane (HBCD) stereoisomers: three diastereomeric pairs of enantiomers

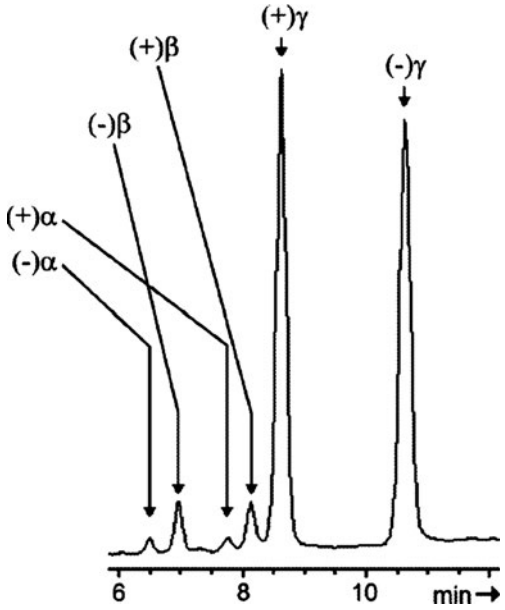

Fig. 2 Separation of the six major HBCD stereoisomers on a chiral permethylated β-cyclodextrin (CD) stationary phase (β-pmCD) column. This figure was taken from [23]

Methods

A computational method for the simulation of elution orders and binding affinities, respectively, should take two aspects into account. First, the conformational flexibility of the compound has to be considered since its binding affinity to the stationary phase or host molecule depends strongly on conformational changes. Although some 3D-QSAR methods incorporate classical force field-based 3D representations of the compound as well [25–27], we decided to use a purely thermodynamic approach by running MD simulations and extracting force field interaction energies for computation of elution order. Also, we avoided methods for the computation of binding free energies, such as the free energy perturbation [28] or thermodynamic integration, that require excessive computational effort [29]. A high-temperature hybrid Monte-Carlo (HMC) run was used in order to find a suitable starting point for our simulations. Second, as mentioned before, an explicit representation of the solvent is desired, because there are several solvents for which implicit modelling is not possible in standard MD-software packages. In our investigations, we applied multi-mode Hamiltonian dynamics simulations.

High-temperature hybrid monte-carlo simulation

Regarding conformational flipping, cyclic compounds including HBCD exhibit high energy barriers that are hard to overcome using ordinary MD simulations. Flipping from one HBCD conformation to another becomes a rare event even if sampled with stochastical methods [30] such as HMC [31], which is known for its efficient sampling of conformational space [32]. For this reason, initial structures for MD simulations as used below need to be chosen very carefully and minimized accordingly. The global conformational minimum should be suitable for our purpose since it is expected to have the largest statistical weight. The isomers were parameterized with the Merck molecular force field (mmff) [33] and simulated for 100 ps applying the HMC method at an artificially high temperature of 1,500 K in order to efficiently sample the conformational space. Each HMC step included 30 MD steps with a 1.3 fs step size. Convergence was checked according to Gelman and Rubin [34] on the basis of five Markov chains. Afterwards, all geometries of the canonical ensemble were minimized with the conjugate gradient method [35, 36], and the lowest energy geometry of all was chosen as the global minimum conformation.

Multi-mode Hamiltonian dynamics simulation

The β-pmCD crystal structure was retrieved from the Cambridge Structural Database (CSD) [37] under the ID COYXET20 [38]. All molecules were parameterized according to the generalized AMBER force field (GAFF) [39] using Antechamber from the AmberTools package v1.4 [40]. Charges were assigned with the am1bcc method [41, 42] designed to reproduce restrained electrostatic potential (RESP) charges [43]. Using the Gromacs v.4.0.4 simulation package [44], each isomer was simulated with two different solvents: once in pure water provided by Amber's ffamber_tip3p model [45], which is included in the GAFF-Gromacs MD interface denoted as AMBER ports [46], and again in pure acetonitrile [47].

As a starting conformation, HBCD was placed into the cavity of β-pmCD, superimposing both geometric centers even though the guest may also interact with the outer face of β-pmCD. Using the nuclear Overhauser effect (NOE) along with nuclear magnetic resonance spectroscopy studies revealed that small hydrophobic and poorly water-soluble compounds like HBCD prefer to reside within the cavity of β-CD [48, 49]. MD simulation was performed in three steps: Initially, the host–guest complex underwent 5,000 steepest descent energy minimization steps if the maximum force did not reach below 100 kJ mol^{-1} nm^{-1} before. During a subsequent 400 ps equilibration phase, all but the solvent's atoms were restrained in their positions. Afterwards, the whole system was simulated for at least 400 ps without position restraints but with constraints on all bonds according to the LINCS approach [50] allowing a discrete step size of 2 fs to be set. In accordance with the HPLC conditions, the temperature of the canonical ensemble was coupled to 303 K by stochastically rescaling atomic velocities [51]. Interaction energies were computed using the Gromacs setting PME-Switch on the basis of the

smooth partical mesh Ewald summation [52] for coulomb potentials with a cutoff at 11 Å, and the shift setting for van der Waals interactions within a dual range switched after 9 Å and cut off at 10 Å.

A set of 60 initial binding modes per isomer was constructed according to the icosahedron's symmetry order as follows: each pair of two opposing vertices provides one rotational axis around which the isomer is rotated in five 72° steps resulting in five binding modes per full circle. Five further orientations associated with the same axis are gained after having swapped the two corresponding vertices by a 180° rotation resulting in ten binding modes per axis. Since there exist five further axes (ten further vertices), each of them providing ten further orientations after having been rotated properly, we arrive at a total number of 60 binding modes. Though this procedure greatly increases computational effort, we are confident that, in contrast to ordinary molecular docking algorithms, we will be able to catch the preferential binding mode(s) (Fig. 3).

Results and discussion

In short, the following steps were performed in order to gain affinity information for the computation of the chromatographic elution order: global minima of the six main stereoisomers were computed and served as initial binding modes for 60 MD simulations per isomer associated with 60 different orientations within the β-pmCD cavity. Having applied three strategies for handling various orientations per isomer, interaction energies between host and guest were computed from the trajectories' equilibrium regions, allowing the relative binding affinities for the six major HBCD stereoisomers to be determined.

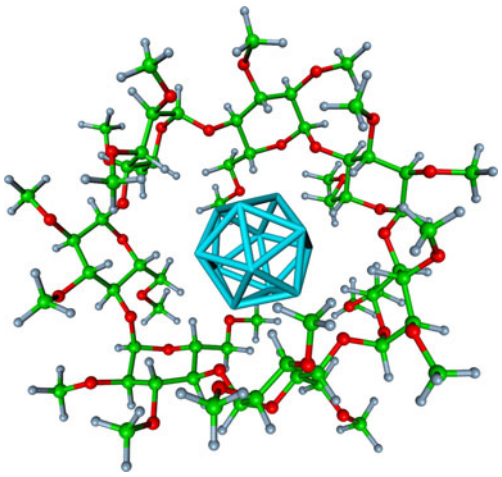

Fig. 3 β-pmCD (NUCLEODEX β-PM) as stationary phase in HPLC analysis. The icosahedron in the β-pmCD cavity represents 60 uniformly distributed rotational binding modes of hexabromocyclododecane providing starting conformations for molecular dynamics (MD) simulations

Computation of global HBCD minima

As depicted in Table 1, the lowest mmff energy values for each enantiomeric pair were identical, indicating a converged conformational sampling. Moreover, after thermal isomerization, the diastereomers displayed an experimental ratio of α:β:γ=81.3:10.0:8.6 [53], correlating closely with the order of computed energies listed in Table 1, which represent most probable geometries within a statistical ensemble.

These and further observations concerning C_2-symmetries of α- and γ-HBCD and minimal energy distributions in torsional subspaces within each canonical ensemble [30] reveal that the conformational space was sampled sufficiently. The crystal structures of α-, β- and γ-HBCD, respectively [54] were retrieved from CSD under the IDs 633325, 617557 and 633326. An alignment of global minima to the respective crystals on the atomic level is shown in Fig. 4. The (+)-β-HBCD geometry matches nearly perfectly, with a torsional root mean square deviation (RMSD) of 0.1 Å (see Table 1), whereas (+)-α-HBCD differs slightly from the crystal. These two diastereomers indicate the high suitability of the mmff fpr the description of molecular conformations. No conformational agreement at all was found in the case of (−)-γ-HBCD. External atomic coordinates were fit to the crystal with an RMSD of 1.1 Å suggesting similar geometries. In contrast, the internal (torsional) distance 108.5° reveals a completely different conformation for (−)-γ-HBCD. This discrepancy might occur due to solvent artefacts in the crystal upon the crystallization process, or due to the fact that the crystal structure does not need to match the global minimum structure.

Simulation performance in water and acetonitrile

A reasonable question concerns the time range of simulation to be considered for further interaction analysis. Figure 5 shows Matlab-smoothed [by its filtfilt() function] distances between HBCD and β-pmCD mass centers during simulation in water (left subfigure) in comparison to ACN (right subfigure). The HBCD orientations shown here were approved as predominant for the reasons specified below.

Because of the high repulsive forces within the β-pmCD cavity, all simulations show a rapid, initial increase in the guest–host distance until an equilibrium is reached after 30–60 ps in the case of water with only small fluctuations of about 0.5 Å within the remaining trajectory. On account of this, the first 80 ps of simulation were omitted when computing average interaction energies. HBCD runs performed with ACN exhibit inconsistent distances showing sudden jumps even after 0.5 ns. This observation might be

Table 1 Global energy minima and root mean square deviation (RMSD) values for the alignment of simulated optimal conformations compared to crystal structures. *HBCD* 1,2,5,6,9, 10-Hexabromocyclododecane

Stereoisomer	Global minimum $\left[\frac{kJ}{mol}\right]$	Cartesian RMSD [Å]	Torsional RMSD [°]
(−)-α-HBCD	238.7	0.5	30.6
(−)-β-HBCD	249.5	–	–
(−)-γ-HBCD	256.7	1.1	108.5
(+)-α-HBCD	238.7	–	–
(+)-β-HBCD	249.5	0.1	0.1
(+)-γ-HBCD	256.7	–	–

due to a more even damping effect of water, which is much lighter and appears at a higher molar density in the surrounding medium than ACN. Mass center distances averaged over time, orientations and isomers after 400 ps are significantly larger in ACN than in water (8.0 Å vs 5.2 Å) confirming the hydrophobic character of HBCD and the assumption that chromatographic separation (interaction with the stationary phase) is more likely in water, whereas solubility, and thus, HBCD elution rate, is higher in more hydrophobic solvents like ACN. Indeed, mean HBCD interaction energies in pure solvents without β-pmCD were computed substantially lower for ACN (−170.7 kJ mol^{-1}) than for water (−148.5 kJ mol^{-1}). However, comparing absolute energy values describing the interaction of a compound with two different surrounding solvents requires caution. Typical low energy modes of (−)-γ-HBCD (smallest distance) and (+)-β-HBCD (largest distance) isomers within β-pmCD simulated in water are depicted in Fig. 6. At equilibrium, about half of each isomers' shape is surrounded by C2-and C3-methoxy moieties of β-pmCD glucopyranose units. Despite this, HBCD interaction is measurable with the entire cyclodextrin molecule since nearly all intermolecular carbon distances are below 10 Å.

Optimal binding mode analysis

Sampling the conformational space completely in order to compute the binding free energy of host-guest complexes at chemical equilibrium is hindered by high energetic barriers. This handicap was accomplished by using several (N=60) binding modes for independent simulations which in turn raise the question of how to select the optimal one of any mode i for each isomer. Therefore, three different strategies E_{mean}, E_{min} and E_{prob} have been compared in order to handle the potential energy $E^i(q_j)$ of conformation q at time step j out of n=160,000 MD steps (after having omitted the first 40,000 steps):

$$E_{\text{min}} = \min_{i\in[1,N]}\left(\frac{1}{n}\sum_{j=1}^{n}E^i(q_j)\right) \tag{1}$$

$$E_{\text{min}} = \min_{i\in[1,N]}\left(\min_{j\in[1,n]}E^i(q_j)\right) \tag{2}$$

$$E_{prob} = -\frac{1}{\beta}\ln\left(\frac{1}{N}\sum_{i=1}^{N}\exp\left(\frac{\beta}{n}\right)\sum_{j=1}^{n}E^i(q_j)\right) \tag{3}$$

As a first approach (Eq. 1), the lowest of all 60 time-averaged energies was assigned to E_{mean}. In Eq. 2, the orientation associated with the lowest energy E_{min} of all 60 minimal energies was chosen. Finally, all orientations were taken into account by summing up their time-averaged energies weighted according to the Boltzmann probability distribution for canonical ensembles yielding E_{prob}. Here, β

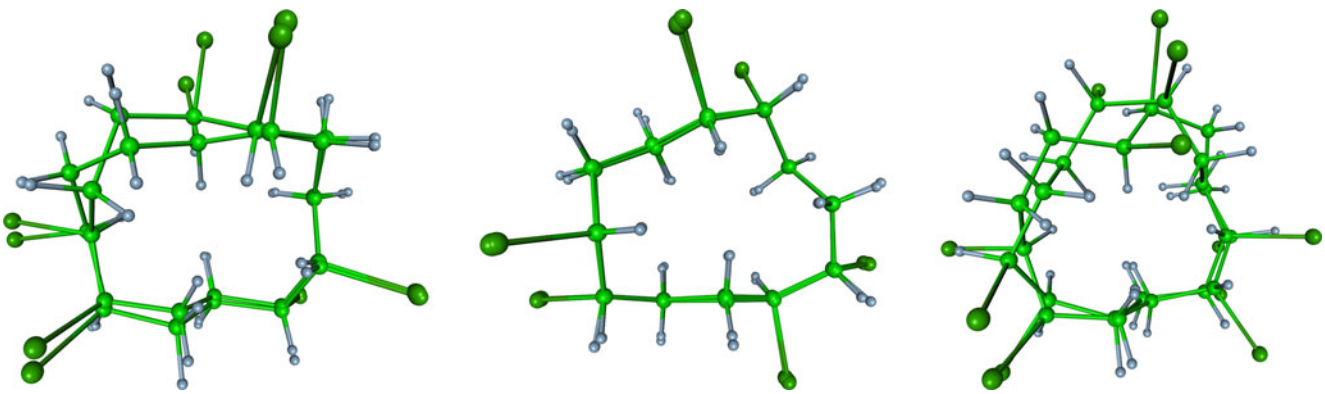

Fig. 4 Alignment of globally minimized main HBCD conformations to their respective X-ray crystallographic structures. From *left* to *right*: α, β, γ diastereomers

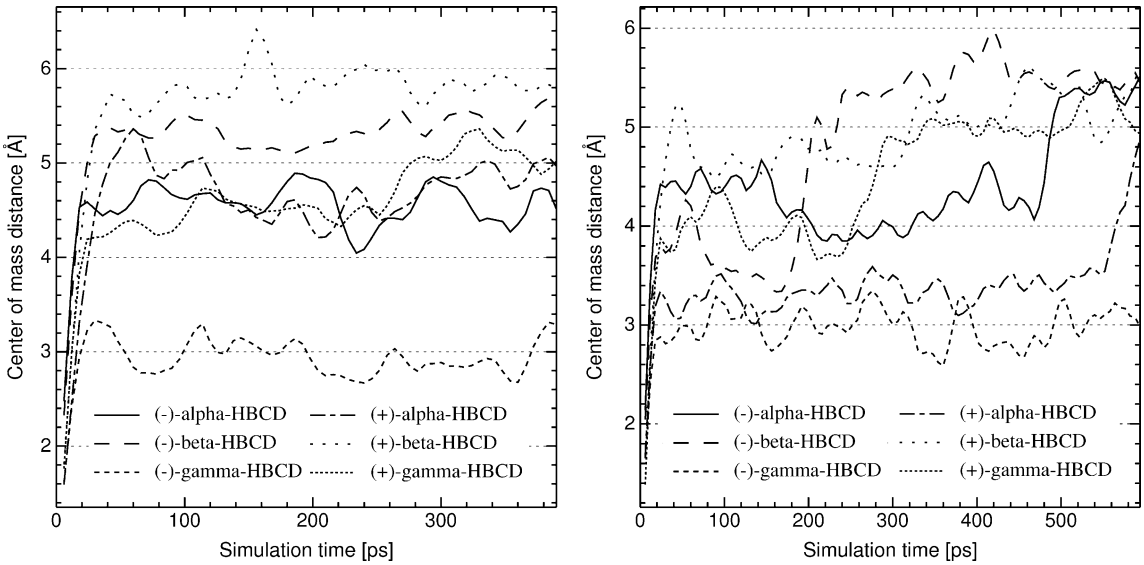

Fig. 5 Center of mass distances between HBCD stereoisomers and β-pmCD in water (*left*) and acetonitrile (*right*)

stands for the inverted product of the gas constant R= 8.31447 J mol^{-1} K^{-1} and temperature T=303 K. Clearly, E_{mean} and E_{prob} cope with thermodynamic principles since they incorporate the mean inner energy of statistical ensembles. In contrast, E_{min} represents molecular docking approaches where affinities are estimated on the basis of an individual preferential binding mode only.

Essential energy contributions

Besides defining strategies for selecting optimal orientations, those energy terms that contribute considerably to the correlation between the simulated and the experimental elution order need to be determined. In a thermodynamic manner, one would rather use the total inner energy of a molecular system for the computation of free energy differences. Due to the high number of water molecules, the inner energy reveals high fluctuations and is therefore neither expected to be reproducible nor to correlate well with the experimental elution order. For this reason, only the sum of all interaction energies (van der Waals and electronic terms) of HBCD with its surroundings (solvent and β-pmCD) was assigned to E^i (qj) in order to compute the enthalpic part of the free energy. This physically meaningful approach has already been applied successfully to the estimation of binding affinities for host–guest systems as provided by the linear interaction energy (LIE) method proposed by Åquist et al. [55].

Table 2 shows squared coefficients for the correlation of the natural logarithm ln(k) of experimental HPLC capacity factors, k, with the sum of interaction energy terms computed in accordance with the three strategies described above. These capacity factors $k_i = (t_i - t_0)/t_0$ had been derived from respective HPLC retention times t_i of isomer i and the chromatographic dead time t_0 depending on all physical properties influencing the retention time [23]. Taking the natural logarithm of k is justified by thermodynamic studies of the chromatographic retention behavior revealing a linear correlation between ln(k) and thermodynamic quantities such as the inversed temperature, the

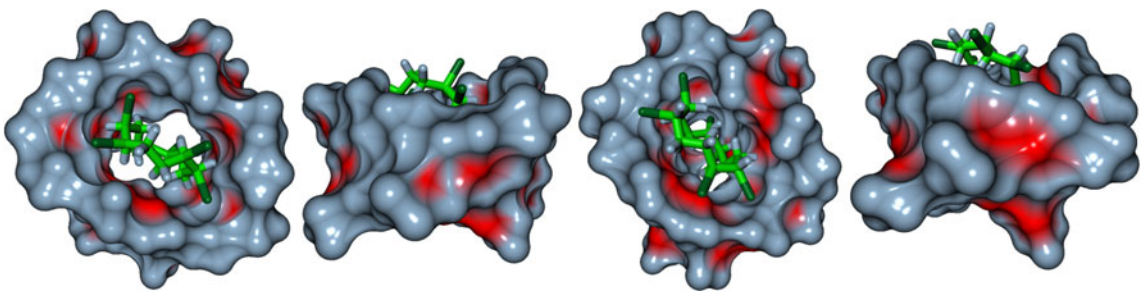

Fig. 6 Low energy conformations of (−)-γ-HBCD within the β-pmCD (represented by its solvent-excluded surface) cavity with a mass center distance of 3 Å on the left-hand and of (+)-β-HBCD with a distance of 5.8 Å on the right-hand fetched from the equilibrium region of an MD simulation with explicit water

Table 2 Squared Pearson coefficients R^2 (three approaches) for the correlation of the natural logarithm of experimental capacity factors with HBCD interaction energies regarding its chemical environment averaged over various time ranges of the MD. The two solvents and the discriminating power for all isomers (*Iso.*) and for enantiomers (*Ena.*) only can be distinguished. *ACN* Acetonitrile

Solvent	$\langle R^2(E_{mean})\rangle$		$\langle R^2(E_{\min})\rangle$		$\langle R^2(E_{prob})\rangle$	
	Iso.	Ena.	Iso.	Ena.	Iso.	Ena.
ACN	0.64	0.31	0.63	0.11	0.67	0.11
Water	0.86	1.00	0.80	1.00	0.87	1.00

enthalpy and free energy [56, 57]. In order to figure out the correlation model's robustness, these coefficients were averaged over multiple time ranges starting at succeeding time frames with 20 ps offsets, but all ending at 360 ps. Additionally, we distinguished between both solvents and the discriminating power for both the entire set of stereoisomers (Iso.) and among enatiomers (Ena.) only. Correlation for enantiomer-specific separation was computed by $R^2(\text{Ena.}) = \frac{1}{3}\left(R_\alpha^2 + R_\beta^2 + R_\gamma^2\right)$.

As a general observation, the coefficients R^2 of correlation computed with Eqs. 1–3 do not differ considerably. However, the choice of the solvent does make a notable difference. With ACN it was not possible to achieve such a high corrrelation with any formula. This observation copes with the experiment since better HBCD separation is achieved with high water concentrations in the eluent whereas elevated ACN concentrations reduce separation but enhance elution of HBCD isomers. The optimal result for the solvent water is showcased in Fig. 7, where correlations have been plotted against the starting frame of the trajectories' time ranges ending at frame t=400 ps. We arrived at consistently high squared correlation coefficients equal to 0.8 if choosing $E_{\min}$ or even better at about 0.86 or 0.87 using one out of equations E_{mean} or E_{prob}, respectively (left diagram). Enantiomer-specific separation (right diagram) in water was estimated exactly over nearly the full range of the MD trajectories by all approaches. Comparing both thermodynamically motivated optimal interaction energies E_{mean} and E_{prob} reveals a sufficient approximation of the Boltzmann-weighted sum of all orientations by the preferential orientation with the highest statistical weight only. These results clearly approve the robustness of our thermodynamic multi-mode approach at least for this hydrophobic class of compounds separated on a stationary phase consisting of host-like molecules. The system's thermodynamic equilibrium is well reflected by coefficients of correlation, which have a consistently high value independent of the time range under consideration. It should be noted that the likeliness for randomly chosing the right order among three independent pairs (enantiomeric separation of HBCD) is indeed $P=0.5^3=0.125$, whereas guessing the order among six stereoisomers is about 100 times more unlikely with $P=(6!)^{-1}=0.0014$.

Computation of the HBCD elution order

A quanitative translation of energy values into chromatographic retention times is impossible since these depend on many parameters such as flow rate, temperature, column length, density and diameter and pressure. However, the estimation of the relative order of elution seems an achievable goal and is the information needed by the analyst. For the estimation of the elution order, all MD trajectories have been considered with water as solvent and within the range from 80 ps through 400 ps as justified on the basis of the mass center distances shown in Fig. 5. Using the least-squares method, optimal interaction energies from all approaches were scaled and shifted in order to minimize the deviation from ln(k). Then, selecting orientations associated with

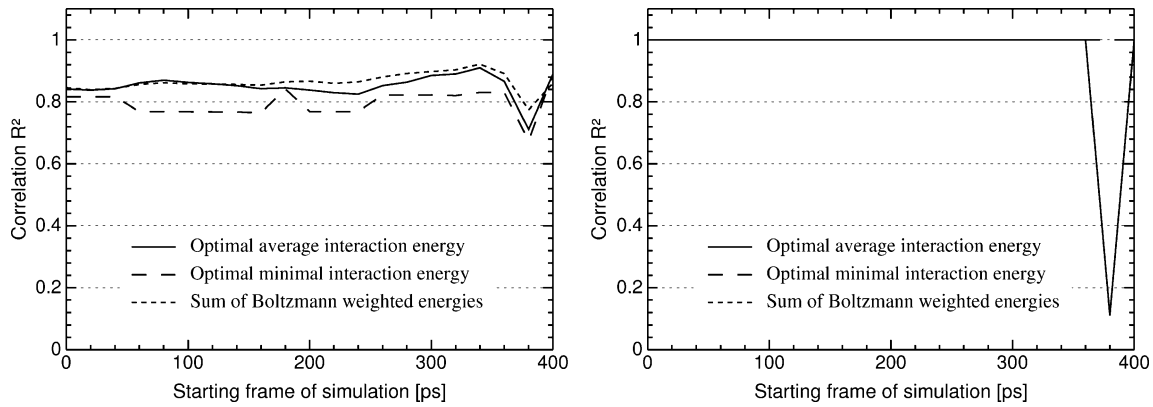

Fig. 7 Squared coefficients for the correlation of HBCD capacity factors with interaction energies depending on the starting frame and simulated in explicit water. Three strategies have been compared for the computation of the elution order for all stereoisomers (*left*) and for three pairs of enantiomers only (*right*)

Table 3 Simulated optimal interaction energies on a β-pmCD stationary phase along with capacity factors and the corresponding elution order from both the HPLC experiment [23] and by least-squares-fitting of optimal interaction energies

Diastereomer	Interaction energy $\left[\frac{kJ}{mol}\right]$			Capacity factor k				Elution order			
	E_{mean}	E_{min}	E_{prob}	HPLC	E_{mean}	E_{min}	E_{prob}	HPLC	E_{mean}	E_{min}	E_{prob}
(–)-α-HBCD	−200.2	−247.1	−28.6	10.01	10.83	11.42	10.84	1	1	2	1
(–)-β-HBCD	−201.9	−241.7	−29.1	10.80	11.11	10.60	11.39	2	2	1	2
(–)-γ-HBCD	−231.7	−275.6	−33.5	17.02	17.47	16.92	17.60	6	6	6	6
(+)-α-HBCD	−207.1	−255.6	−29.8	12.16	12.02	12.84	12.21	3	4	5	4
(+)-β-HBCD	−205.9	−247.6	−29.4	12.79	11.80	11.50	11.74	4	3	3	3
(+)-γ-HBCD	−209.3	−253.6	−30.1	13.62	12.43	12.49	12.58	5	5	4	5

optimal mean inner energies E_{mean} of all interaction terms summed up yields a squared coefficient of correlation R^2= 0.87, which is slightly higher than R^2=0.86 achieved by the Boltzmann-weighted approach E_{prob}, and considerably higher than R^2=0.77 computed with the single-step approach E_{min}. These squared coefficients increase to 0.92, 0.91, and 0.82, respectively, if the energies are fitted to k instead of ln(k). The correlation function 4 is exemplified using E_{mean}, which contributed the highest correlation:

$$\ln(k) = -0.0152\frac{\text{mol}}{\text{kJ}}E_{mean} - 0.6614, \tag{4}$$

which can be rearranged easily in order to obtain an estimated k instead of ln(k) for comparison with experimental k *values*

$$k = \exp\left(-0.0152\frac{\text{mol}}{\text{kJ}}E_{mean} - 0.6614\right). \tag{5}$$

Experimental (HPLC) capacity factors k and elution orders [23] are listed in Table 3 along with those attained by fitting optimal interaction energies to ln(k). E_{mean} also achieved the highest squared rank correlation (according to Spearman) of estimated and HPLC data $R_S^2 = 0.89$ as well as the highest squared cofficient $R_{LOO}^2 = 0.72$ upon the leave-one-out (LOO) cross-validation for evaluating the model, which even amounts to $R_{LOO}^2 = 0.81$ when neglecting the constant term in the correlation Eq. 4. During the cross-validation, for each isomer, ln(k) was predicted on the basis of the isomers left over as training set. In detail, the training set's computed energies E_{mean} were fitted to the respective subset of HPLC capacity factors ln(k) using least-squares, and resulting in a slope and an intercept. In turn, these coefficients were applied to the mapping of the excluded isomer's energy E_{mean} to theoretical capacity factors ln(k). Afterwards, the squared coefficient R_{LOO}^2 was determined by analogy to R^2 using these estimated values of ln(k) for the correlation analysis instead of E_{mean}.

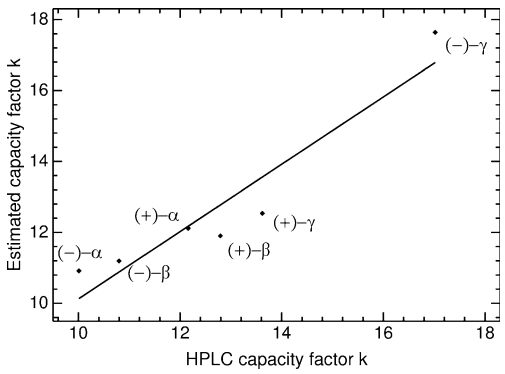

Fig. 8 Correlation of amber force field interaction energies (after least-squares fitting) with HBCD stereoisomers' capacity factors from chiral HPLC separation [23]

Figure 8 shows experimental capacity factors k plotted against those estimated on the basis of E_{mean}. Interestingly, by far the highest affinity was estimated correctly for (−)-γ-HBCD, which is indeed eluted a noticeable time period after all other stereoisomers, as sketched in the chromatogram (Fig. 2). Moreover, the smallest difference Δk=0.63 in HPLC capacity factors [and Δln(k), respectively] between any pair of two stereoisomers is the one between the (+)-α and (+)-β stereoisomer correlating with the smallest differences ΔE_{mean}=1.2 kJ mol^{-1} and ΔE_{prob}= 0.4 kJ mol^{-1} in optimal interaction energies derived from both mean inner energy-based methods and possibly explaining the only failure in the computed elution order associated with these two isomers. However, enantiomer-specific separation was estimated correctly with all approaches in explicit water. It should be noted that chromatographic separation in pure water or pure ACN does not yield different orders of elution and does not lead to separation of all six stereoisomers. Already for this reason, we cannot expect an exact agreement with the simulation. Regarding the three strategies used to handle the multiple binding modes for affinity analysis, statistical approaches on the basis of mean potential energies turn out to be more convenient than single-geometry approaches such as E_{min}.

Conclusion and outlook

Considerable cross-validated correlations of simulated interaction energies incorporating multiple binding modes with the chromatographic elution order of HBCD stereoisomers have been achieved using water as solvent and considering all HBCD interactions with its surroundings, which are dominated by the hydrophobic Lennard-Jones potential. Considering especially both mean inner energy-based scoring functions reveals consistently high correlations of all isomers' computed elution order with the experimental order, regardless of the time range under consideration and yielding an exactly estimated order of enantiomer-specific elution. Comparing both mathematical approaches indicates a sufficient approximation of the Boltzmann-weighted sum of all orientations by considering the most favorable binding mode only. On the face of these results, the presented multi-mode approach could help with the estimation of binding affinities for host–guest systems without binding mode information. Our strategy was well exemplified by simulating the elution order of chromatographic separation and might be useful whenever experimental assignment of peaks to stereoisomers is impossible or for selecting suitable stationary phases for a given mixture of compounds. In general, binding affinity estimation for other host–guest systems such as receptor–ligand or enzyme–substrate complexes, could benefit from systematic consideration of the space of orientations.

Acknowledgment The BAM Federal Institute for Material Research and Testing is kindly acknowledged for its cooperation and financial support.

References

1. Zhang G, Sun Q, Hou Y, Hong Z, Zhang J, Zhao L, Zhang H, Chai Y (2009) J Sep Sci 32:2401–2407
2. Issaraseriruk N, Shitangkoon A, Aree T (2010) J Mol Graphics Modell 28:506–512
3. Morris GM, Goodsell DS, Halliday RS, Huey R, Hart WE, Belew RK, Olson AJ (1998) J Comput Chem 19:1639–1662
4. Stewart JJP (1989) J Comput Chem 10:209–220
5. Pérez-Garrido A, Helguera AM, Cordeiro MND, Escudero AG (2009) J Pharm Sci 98:4557–4576
6. Alvira E, Mayoral JA, García JI (2008) J Incl Phenom Macrocycl Chem 60:103–113
7. Lipkowitz KB, Pearl G, Coner B, Peterson MA (1997) J Am Chem Soc 119:600–610
8. Barda HJ, Sanders DC, Benya TJ (1985) Bromine compounds. In: Hawkins S, Schultz G (eds) Ullmann's Encyclopedia of Industrial Chemistry. Wiley-VCH, Weinheim, pp 405–429
9. BSEF. Bromine Science and Environmental Forum. http://www.bsef.com/oursubstances/hbcd/about-hbcd/. Accessed 29 July 2010
10. de Witt CA (2002) Chemosphere 46:583–624
11. Law RJ, Allchin LC, de Boer J, Covaci A, Herzke D, Lepom P, Morris S, Tronczynski J, de Witt CA (2006) Chemosphere 64:187–208
12. de Witt CA, Alaee M, Muir DCG (2006) Chemosphere 64:209–233
13. Covaci A, Gerecke ASC, Voorspoels RJLS, Kohler M, Heeb NV, Leslie H, Allchin CR, DeBoer J (2006) Environ Sci Technol 40:3680–3688
14. Köppen R, Becker R, Esslinger S, Nehls I (2010) Chemosphere 80:1241–1245
15. Esslinger S, Becker R, Jung C, Schröter-Kermani C, Bremser W, Nehls I (2011) Chemosphere 83:161–167
16. Vos JG, Becher G, van den Berg M, de Boer J, Leonards PEG (2003) Pure Appl Chem 75:2039–2046
17. Hamers T, Kamstra JH, Sonneveld E, Murk AJ, Kester MHA, Andersson PL, Legler J, Brouwer A (2006) Toxicol Sci 92:157–173
18. Meerts IATM, van Zanden JJ, Luijks EAC, van Leeuwen-Bol I, Marsh G, Jakobsson E, Bergman A, Brouwer A (2000) Toxicol Sci 56:95–104
19. Peled M, Scharia R, SondackD (1995) Thermal rearrangement of hexabromo-cyclododecane (HBCD). In: Desmurs JR, Gérard B, Goldstein MJ (eds) Advances in organobromine chemistry II. Elsevier, Amsterdam, pp 92–99
20. Janák K, Covaci A, Voorspoels S, Becher G (2005) Environ Sci Technol 39:1987–1994
21. Janák K, Sellström U, Johansson AK, Becher G, de Witt CA, Lindberg P, Helander B (2008) Chemosphere 73:193–200
22. Tomy GT, Pleskach K, Oswald T, Halldorson T, Helm PA, Macinnis G, Marvin CH (2008) Environ Sci Technol 42:3634–3639
23. Köppen R, Becker R, Emmerling F, Jung C, Nehls I (2007) Chirality 19:214–222
24. Heeb NV, Schweizer WB, Kohler M, Gerecke AC (2005) Chemosphere 61:65–73
25. Tokarski JS, Hopfinger AJ (1997) J Chem Inf Comput Sci 37:792–811
26. Hopfinger AJ, Tokarski JS (1997) 3D-QSAR analysis. In: Charifsom PS (ed) Practical applications of computer-aided drug design. Dekker, New York
27. Ortiz AR, Pisabarro MT, Gago F, Wade RC (1995) J Med Chem 38:2681–2691
28. Zwanzig RW (1954) J Chem Phys 22:1420–1426
29. Kirkwood JG (1935) J Chem Phys 3:300–313
30. Weber M, Becker R, Durmaz V, Köppen R (2008) Mol Simul 34:727–736
31. Duane S, Kennedy AD, Pendleton BJ, Roweth D (1987) Phys Lett B 195:216–222
32. Brass A, Pendleton BJ, Chen Y, Robson B (1993) Biopolymers 33:1307–1315
33. Halgren TA (1996) J Comp Chem 17(5–6):490–519
34. Gelman A, Rubin D (1992) Statist Sci 7:457–511
35. Hestenes MR, Stiefel E (1952) J Res Nat Bur Stand 49:409–436
36. Fletcher R, Reeves CM (1964) Comput J 7:149–154
37. Allen FH (2002) Acta Crystallogr B58:380–388
38. Harata K, Uekama K, Imai T, Hirayama F, Otagiri M (1988) J Inclusion Phenomena 6:443–460
39. Wang J, Wolf RM, Caldwell JW, Kollman PA, Case DA (2004) J Comput Chem 25:1157–1174
40. Wang J, Wang W, Kollman PA, Case DA (2006) J Mol Graphics Modell 25:247–260
41. Jakalian A, Bush BL, Jack DB, Bayly CI (2000) J Comput Chem 21:132–146
42. Jakalian A, Jack DB, Bayly CI (2002) J Comput Chem 23:1623–1641
43. Cornell WD, Cieplak P, Bayly CI, Kollman PA (1993) J Am Chem Soc 115:9620–9631
44. Hess B, Kutzner C, van der Spoe D, Lindahl E (2008) J Chem Theory Comput 4:435–447

45. Jorgensen WL, Chandrasekhar J, Madura JD (1983) J Chem Phys 79:926–935
46. Sorin EJ, Pande VS (2005) Biophys J 88:2472−2493
47. Nikitin AM, Lyubartsev AP (2007) J Comput Chem 28:2020–2026
48. Wang J, Warner IM (1993) Microchem J 48:229–239
49. Redondo J, Frigola J, Torrens A, Lupón P (1995) Magn. Res. Chem J 33:104–109
50. Hess B, Bekker H, Berendsen HJC, Fraaije JGEM (1997) J Comp Chem 18:1463–1472
51. Bussi G, Donadio D, Parrinello M (2007) J Chem Phys 126:014101
52. Essmann U, Perera L, Berkowitz ML (1995) J Chem Phys 103:8577–8593
53. Köppen R, Becker R, Jung C, Nehls I (2008) Chemosphere 71:656–662
54. Heeb NV, Schweizer WB, Mattrel P, Haag R, Gerecke AC, Kohler M, Zennegg PSM, Wolfensberger M (2007) Chemosphere 68:940–950
55. Åquist J, Medina C, Samuelsson JE (2008) Protein Eng 60:103–113
56. McGachy NT, Grinberg N, Variankaval N (2005) J Chromatogr A 1064:193–204
57. Shi JH, Ding ZJ, Hu Y (2011) Chromatographia 74:319–325